

# Local Factors Modulate Tissue-Specific NEFA Utilization

## Assessment in Rats Using $^3\text{H}$ -(R)-2-Bromopalmitate

Stuart M. Furler, Gregory J. Cooney, Bronwyn D. Hegarty, Megan Y. Lim-Fraser, Edward W. Kraegen, and Nicholas D. Oakes

**Insulin-resistant states are associated with accumulation of muscle lipid, suggesting an imbalance between lipid uptake and oxidation. We have employed a new fatty-acid tracer [9,10- $^3\text{H}$ ](R)-2-bromopalmitate ( $^3\text{H}$ -R-BrP) to study individual-tissue nonesterified fatty acid (NEFA) uptake in states with diminished or enhanced lipid oxidation.  $^3\text{H}$ -R-BrP was administered to conscious male Wistar rats (~300 g) during fasting (5, 18, or 36 h), acute blockade of  $\beta$ -oxidation (etomoxir, 15  $\mu\text{mol}/\text{kg}$ ), and insulin infusion (0.25  $\text{U} \cdot \text{kg}^{-1} \cdot \text{h}^{-1}$ ). Estimates of NEFA clearance rates ( $K_f^*$ ) and absolute rates of uptake ( $R_f^*$ ) were calculated from tissue accumulation of  $^3\text{H}$ -R-BrP products. In the basal state, NEFA uptake was dependent on the oxidative capacity of tissues:  $R_f^*$  in brown adipose tissue (BAT) > heart (HRT) > diaphragm (DPHM) > red quadriceps (RQ) > white quadriceps (WQ) > white adipose tissue (WAT). Fasting increased ( $P < 0.001$ )  $K_f^*$  in WAT but did not change NEFA clearance in other tissues. However, plasma NEFA levels were raised ( $P < 0.01$ ), tending to elevate  $R_f^*$  in most tissues ( $P < 0.05$ : WAT, BAT, WQ, DPHM). Etomoxir reduced ( $P < 0.01$ )  $K_f^*$  only in oxidative tissues (BAT, RQ, DPHM, HRT). Insulin lowered plasma NEFA levels ( $P < 0.001$ ) and significantly decreased  $R_f^*$  in most tissues ( $P < 0.05$ : WAT, RQ, DPHM, HRT). An increased ( $P < 0.05$ ) clearance was observed in WAT, BAT, and WQ; a decrease ( $P < 0.01$ ) in  $K_f^*$  was observed in HRT. This study is the first to measure tissue-specific NEFA uptake in conscious rats in the postabsorptive, fasted, and insulin-stimulated states. We have demonstrated that tissue NEFA utilization is not exclusively determined by systemic availability, but that the early steps of NEFA uptake or metabolic sequestration can also be rapidly modulated by local processes such as NEFA oxidation. *Diabetes* 49:1427-1433, 2000**

From the Diabetes & Metabolism Research Program (S.M.F., G.J.C., B.D.H., M.Y.L.-F., E.W.K.), Garvan Institute of Medical Research, Sydney, New South Wales, Australia; and Preclinical Research (N.D.O.), AstraZeneca Research and Development, Mölndal, Sweden.

Address correspondence and reprint requests to Stuart M. Furler, PhD, Garvan Institute of Medical Research, St. Vincent's Hospital, 384 Victoria St., Sydney NSW 2010, Australia. E-mail: s.furler@garvan.unsw.edu.au.

Received for publication 3 December 1999 and accepted in revised form 30 May 2000.

$^3\text{H}$ -R-BrP, [9,10- $^3\text{H}$ ](R)-2-bromopalmitate;  $^{14}\text{C}$ -P, [ $^{14}\text{C}$ ]palmitate; ANOVA, analysis of variance;  $K_f^*$ , clearance rate of  $^3\text{H}$ -R-BrP by individual tissues;  $K_{14}^*$ , clearance rate of  $^{14}\text{C}$ -P by individual tissues; NEFA, nonesterified fatty acid;  $R_f^*$ , total tissue NEFA utilization.

Evidence continues to amass that increased intracellular fatty acid availability (particularly in skeletal muscle) is intimately linked to insulin resistance (1,2) and a range of disease states, including type 2 diabetes (3). Intracellular lipid accumulation could result from modifications to a number of biochemical processes, including accelerated entry of nonesterified fatty acid (NEFA) into the cell, elevated rates of triglyceride formation, or impaired lipid oxidation. However, it is currently unclear whether the lipid accumulation is the cause or the result of the insulin resistance (1).

We have recently developed a novel tracer methodology, based on [9,10- $^3\text{H}$ ](R)-2-bromopalmitate ( $^3\text{H}$ -R-BrP), to quantify the rate of tissue utilization of plasma NEFA in laboratory rats. The fatty-acid analog  $^3\text{H}$ -R-BrP has access to the cytosol and is a substrate for the initial acylation process, but it is not oxidized in the mitochondria (4). Because the metabolic products of  $^3\text{H}$ -R-BrP are not rapidly exported (5), the tissue accumulation of radio-label, following systemic administration, can be used to estimate NEFA uptake. This methodology was designed to determine total (oxidation and storage) NEFA uptake. In contrast, the recently introduced tracer fluoro-6-thia-heptadecanoic acid (used in positron emission tomography studies) is predominantly an indicator of oxidation (6). The initial validation studies of  $^3\text{H}$ -R-BrP were performed in anesthetized rats (5). Here we extend the use of this tracer technique to conscious animals.

We have studied the effects of fasting, etomoxir (a pharmacological inhibitor of NEFA  $\beta$ -oxidation), and hyperinsulinemia. It is well established that these 3 treatments modulate whole-body lipid oxidation (7-10). Here, we have investigated tissue-specific responses to characterize the link between oxidation and uptake and to delineate potential mechanisms of lipid accumulation. Our studies reveal that, apart from systemic NEFA availability, tissue NEFA uptake is dependent on local tissue factors, including the rate of  $\beta$ -oxidation.

### RESEARCH DESIGN AND METHODS

**Animals.** The experiments described here were approved by the Garvan Institute/St. Vincent's Hospital Animal Experimentation Ethics Committee, following guidelines issued by the National Health and Medical Research Council (Australia).

Experiments were performed on male Wistar rats (weight ~300 g), purchased from Animal Resources Centre, Perth, Western Australia. Rats were housed in a temperature-controlled ( $22 \pm 1^\circ\text{C}$ ) environment with a 12:12 h

light:dark cycle (lights on at 0600) with free access to commercial rodent diet (Norco, Kempsey, Australia) and water. One week before study, chronically indwelling cannulas were inserted into the jugular vein and carotid artery under ketamine hydrochloride (90 mg/kg) and xylazine (10 mg/kg) anesthesia as previously described (11). After surgery, rats were housed in individual cages and allowed to recover for 7–10 days. Only rats that had regained their preoperation weight by this time were studied.

**Treatment before tracer administration.** To study fasting periods of varying lengths, food, but not water, was removed from animal cages either 5, 18, or 36 h before the acute investigation period, which commenced at 1000. Five-hour fasted rats are in the postabsorptive state and are routinely used as control animals (12).

Some rats were given a large dose of ethyl-2-[6-(4-chlorophenoxy)-hexyl]oxirane-2-carboxylate (etomoxir), a carnitine palmitoyl transferase I inhibitor, to completely block  $\beta$ -oxidation or insulin. Etomoxir (15  $\mu$ mol/kg; RBI, Natick, MA) was injected intravenously 30 min before commencement of the tracer infusion. Insulin (Actrapid; Novo-Nordisk, Copenhagen, Denmark) was infused into the jugular cannula at a constant rate of 0.25 U  $\cdot$  kg<sup>-1</sup>  $\cdot$  h<sup>-1</sup>, together with a variable-rate glucose infusion to maintain plasma glucose levels (12). Tracer was not administered until a stable euglycemic-hyperinsulinemic state was established, typically 90 min after commencement of the insulin infusion.

The effects of etomoxir were studied in rats fasted for 5 and 18 h. Insulin was administered to postabsorptive animals only. In all, 6 groups of rats were used. Treatment profiles for each group are summarized in Table 1.

**Tracer administration.** Rats were administered a mixture of <sup>3</sup>H-R-BrP and [U-<sup>14</sup>C]palmitate (<sup>14</sup>C-P). The <sup>3</sup>H-R-BrP tracer was produced by AstraZeneca Mölndal, Sweden. The synthesis of racemic [9,10-<sup>3</sup>H]-2-bromopalmitic acid and subsequent resolution of the R-isomer has been previously described (5). The <sup>14</sup>C-P tracer was commercially available (Dupont, Boston, MA). Each rat was infused with  $\sim 50 \times 10^6$  dpm <sup>3</sup>H-R-BrP and  $\sim 30 \times 10^6$  dpm <sup>14</sup>C-P in 1 ml of vehicle. Tracer was delivered in saline conjugated with bovine serum albumin (5). The albumin-tracer complex was infused at a constant rate into the jugular cannula of conscious rats over a 4-min period.

Apart from calculation of rates of whole-body NEFA turnover, the only purpose of administering <sup>14</sup>C-P tracer in the present study was to quantify the relationship between tissue clearance rates of this authentic NEFA and the analog <sup>3</sup>H-R-BrP in the conscious state.

**Plasma samples.** To characterize the plasma <sup>3</sup>H-R-BrP and <sup>14</sup>C-P activity time courses, arterial blood samples ( $\sim 200$   $\mu$ l) were collected from the carotid catheter at 1, 2, 3, 4, 5, 6, 8, 12, and 16 min after the start of tracer infusion. To determine hormone and substrate levels, extra blood ( $\sim 200$   $\mu$ l) was collected with the final sample, and an additional sample ( $\sim 400$   $\mu$ l) was taken immediately before initiation of tracer infusion. All blood samples were immediately centrifuged. The separated plasma was quickly frozen by immersion in liquid nitrogen and then stored at  $-20^\circ\text{C}$  until analyzed. Throughout the experiment, the arterial catheter was kept patent by periodic flushing with small quantities of 20 mmol/l sodium citrate in saline.

**Tissue samples.** After collection of the final blood sample, rats were killed with an overdose (60 mg) of pentobarbitone injected into the carotid catheter. Samples of tissues, including white quadriceps, red quadriceps, diaphragm, heart, inguinal white adipose tissue, and intrascapular brown adipose tissue, were rapidly dissected, freeze-clamped with aluminum tongs precooled in liquid nitrogen, and stored at  $-70^\circ\text{C}$  awaiting analysis.

**Plasma tracer concentrations.** A lipid separation procedure (13) was used to isolate <sup>3</sup>H-R-BrP and <sup>14</sup>C-P from total <sup>3</sup>H and <sup>14</sup>C plasma activities. An initial cold lipid extraction, using a mixture of isopropanol-hexane-0.5 mol/l H<sub>2</sub>SO<sub>4</sub> (40:10:1), was followed by a polarity separation step under alkaline conditions. The latter procedure predominantly partitioned neutral lipids (including esterified fatty acids) into a hexane phase and polar lipids (including NEFAs such as the <sup>3</sup>H-R-BrP and <sup>14</sup>C-P tracers) into an alcohol phase. Small corrections (<10%), based on separation of NEFA and esterified fatty acid standards, were applied for incomplete partitioning of tracer (5).

**Tissue tracer content.** Total <sup>3</sup>H and <sup>14</sup>C activities in tissue samples ( $\sim 100$  mg) were measured using a Packard System 387 Automated Sample Preparation Unit (Packard Instrument, Meriden, CT). This instrument completely oxidized the tissue samples and collected the resulting labeled combustion products, <sup>3</sup>H<sub>2</sub>O and <sup>14</sup>CO<sub>2</sub>, in separate vials. The activities of collected <sup>3</sup>H and <sup>14</sup>C were measured individually using single-channel liquid-scintillation protocols (Wallac 1409 counter; Wallac OY, Turku, Finland).

**Plasma substrate and hormone concentrations.** Plasma glucose concentrations were measured by the glucose oxidase method (YSI 2300; YSI, Yellow Springs, OH). Plasma NEFA levels were determined using an acyl-CoA oxidase based colorimetric kit (WAKO NEFA-C; WAKO Pure Chemical Industries, Osaka, Japan). Plasma insulin was determined using a rat insulin radioimmunoassay kit (Linco Research, Charles, MO).

**Calculations.** The clearance rates of <sup>3</sup>H-R-BrP and <sup>14</sup>C-P by individual tissues (K<sub>t</sub><sup>\*</sup> and K<sub>t</sub><sup>'</sup> respectively) were calculated as previously described (5):

$$K_t^* = \frac{m_B}{\int_0^T C_B(t) dt} \quad K_t' = \frac{m_P}{\int_0^T C_P(t) dt} \quad (1)$$

where  $m_B$  and  $m_P$  are the tissue content of radiolabeled products of <sup>3</sup>H-R-BrP and <sup>14</sup>C-P, respectively;  $C_B$  and  $C_P$  are arterial plasma concentrations of extracted <sup>3</sup>H-R-BrP and <sup>14</sup>C-P, respectively; and  $T$  is the length of the experiment ( $\sim 16$  min).

For data from each rat, the initial step in the evaluation of the above integrals was to use nonlinear regression to fit the discrete  $C_B$  and  $C_P$  values to a mathematical model. The 4-parameter model used corresponded (for the truncated infusion protocol used) to a double-exponential impulse response function. Integrals were then evaluated analytically, using best-fit parameter values (5).

An index of total tissue NEFA utilization (R<sub>t</sub><sup>\*</sup>) was calculated from

$$R_t^* = K_t^* \cdot C_{FA} \quad (2)$$

where  $C_{FA}$  is the plasma concentration of cold NEFA.

Estimates of whole-body <sup>14</sup>C-P clearance and NEFA utilization (MCR<sub>p</sub> and R<sub>p</sub>, respectively) were derived from

$$MCR_p = \frac{D}{\int_0^\infty C_P(t) dt} \quad R_p = MCR_p \cdot C_{FA} \quad (3)$$

where  $D$  is the total dose of <sup>14</sup>C-P administered during the 4-min infusion period.

TABLE 1  
Treatment groups and auxiliary variables

	Group					
	Fast (5 h)	Fast (5 h) + EtX	Fast (5 h) + Ins	Fast (18 h)	Fast (18 h) + EtX	Fast (36 h)
Length of fast (hours)	5	5	5	18	18	36
Additional treatment	—	Etomoxir	Insulin	—	Etomoxir	—
n	7	7	5	6	6	6
Body weight (g)	288 ± 9	295 ± 8	310 ± 9	267 ± 3	285 ± 6	280 ± 6
Plasma glucose (mmol/l)	8.3 ± 0.2	7.9 ± 0.2	7.4 ± 0.3*	5.8 ± 0.1	5.7 ± 0.2	6.1 ± 0.1†
Plasma insulin (mU/l)	36 ± 6	30 ± 7	112 ± 12‡	8 ± 2	14 ± 3	6 ± 1§

Concentrations shown are the means derived from 2 plasma samples taken immediately before initiation of tracer administration and cessation of the experiment. Etomoxir (15  $\mu$ mol/kg) was administered 30 min before tracer. Exogenous insulin was infused at 0.25 U  $\cdot$  kg<sup>-1</sup>  $\cdot$  h<sup>-1</sup>. Euglycemia was maintained by clamp. \* $P < 0.05$  (effect of hyperinsulinemia); † $P < 0.01$  (effect of fasting); ‡ $P < 0.001$  (effect of hyperinsulinemia), § $P < 0.001$  (effect of fasting).

The integral in Eq. 3 was evaluated as described above for Eq. 1, except that an infinite upper limit of integration was used.

In this study, estimates of NEFA clearance, as well as absolute uptake of NEFA, are presented. The 2 variables convey different information, and both are useful in interpretation of results. Estimates of  $R_f^*$  provide quantitative descriptions of changes in overall lipid metabolism due to all factors, including variation in the plasma concentration of cold NEFA (Eq. 2). In contrast,  $K_f^*$  estimates are not influenced (Eq. 1) by this potentially confounding effect and therefore provide a tissue-specific index of NEFA metabolism that is less susceptible to whole-body perturbations.

**Statistical analysis.** A separate statistical test was used to detect an overall effect of each of the 3 primary treatments used in the study.

**Fasting.** A Kendall rank correlation was used to test for a consistent trend across data from the 3 groups: Fast (5 h), Fast (18 h), and Fast (36 h).

**Etomoxir.** Data from the 4 groups: Fast (5 h), Fast (5 h) + Etx, Fast (18 h), and Fast (18 h) + Etx (Table 1) were analyzed by 2-way analysis of variance (ANOVA).

**Insulin.** Data from Fast (5 h) and Fast (5 h) + Ins groups were compared by *t* test.

## RESULTS

**General.** The effects of the various treatments on whole-body indexes of NEFA metabolism are shown in Fig. 1. The NEFA turnover data were derived from the plasma kinetics of the authentic NEFA tracer  $^{14}\text{C}$ -P. Indexes of tissue-specific NEFA metabolism derived from  $^3\text{H}$ -R-BrP data are shown in Fig. 2 (absolute uptake) and Fig. 3 (clearance). Prevailing plasma glucose and insulin concentrations are included in Table 1.

**Fasting.** The 3 groups used to assess the effect of fasting are shown in Figs. 1–3 as unfilled columns. Statistically significant trends with length of fast are denoted by a dagger (†) over the right-most bar.

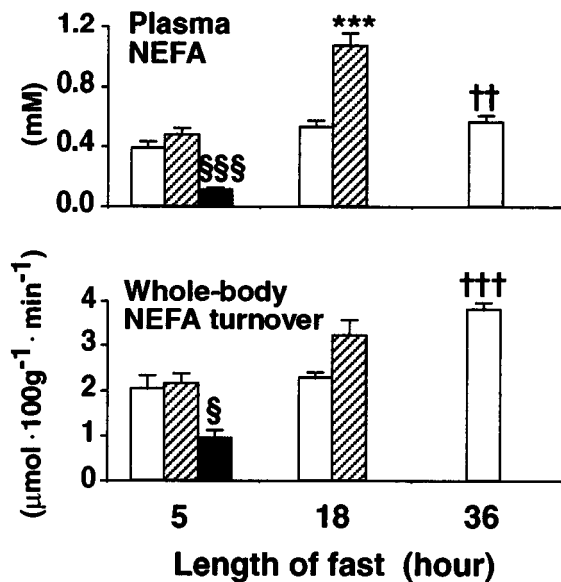


**FIG. 1.** Whole-body indexes of NEFA metabolism for fasted but otherwise untreated rats (□), etomoxir-treated rats (▨), and hyperinsulinemic rats (■). Plasma NEFA concentration for each rat is the mean of 8 readings taken throughout the tracer infusion period. Turnover estimates were derived from the rate of disappearance of palmitate tracer from the plasma and mean NEFA concentration (Eq. 3). \*, †, and § indicate a significant effect of etomoxir administration, fasting, and hyperinsulinemia, respectively.  $§P < 0.05$ ; †† $P < 0.01$ ; †††, §§§ $P < 0.001$ .

Plasma NEFA levels were mildly elevated with fasting (Fig. 1); a concurrent decrease in both glucose and insulin plasma concentrations was also observed (Table 1). There was an increase in whole-body NEFA turnover with fasting (Fig. 1), as progressively more of the body's energy requirements were met by lipid oxidation.

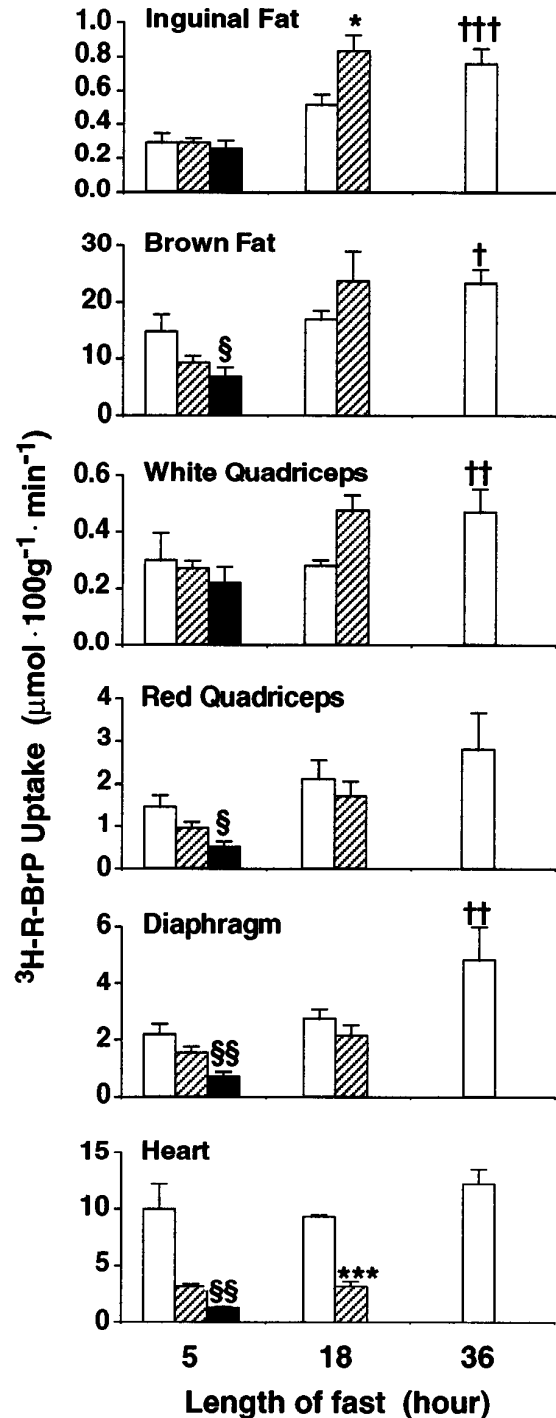


**FIG. 2.** Tissue NEFA uptake rates ( $R_f^*$ ) derived from  $^3\text{H}$ -R-BrP tracer accumulation in fasted but otherwise untreated rats (□), etomoxir-treated rats (▨), and hyperinsulinemic rats (■). \*, †, and § indicate a significant effect of etomoxir administration, fasting, and hyperinsulinemia, respectively. \*, †, § $P < 0.05$ ; ††, §§ $P < 0.01$ ; †††, §§§ $P < 0.001$ .

Elevated plasma NEFA levels would, by mass action alone, tend to increase tissue NEFA uptake. Estimates of NEFA uptake, derived from  $^3\text{H-R-BrP}$  tissue accumulation, increased significantly with fasting in most of the tissues studied (Fig. 2). However, except for white fat (Fig. 3),

there was no detectable change in individual tissue  $^3\text{H-R-BrP}$  clearance, suggesting that any fasting-induced tissue-level alterations in the processes responsible for the uptake and sequestration of NEFA from plasma occur predominantly in the fat depots.

**Pharmacological inhibition of  $\beta$ -oxidation.** Etomoxir was administered to 2 groups of rats that had been fasted for 5 and 18 h, respectively. Etomoxir-treated groups are shown as shaded bars in all figures. One or more asterisks (\*) above the right shaded bar denote a significant main effect of etomoxir administration. These statistical results are derived by 2-way ANOVA and indicate an overall etomoxir effect across both the 5- and 18-h fasted states.

Etomoxir administration elevated plasma NEFA levels, with no detectable change in the rate of whole-body NEFA turnover (Fig. 1). These results reflect blockade of  $\beta$ -oxidation in oxidative tissues but no effect of etomoxir on NEFA appearance rates. The elevation of plasma NEFA was more pronounced in 18-h than in 5-h fasted rats ( $P < 0.001$ , 2-way ANOVA interaction term), which is consistent with increased lipolysis from fat depots and increased tissue dependence on NEFA oxidation as the fasting period was increased.

As shown in Fig. 3, etomoxir significantly reduced  $^3\text{H-R-BrP}$  clearance in oxidative tissues (brown fat, red quadriceps, diaphragm, and heart), but not in nonoxidative tissues (inguinal fat and white quadriceps).

Absolute NEFA uptake ( $R_f^*$ ) was calculated as the product of clearance and circulating NEFA levels (Eq. 2). Etomoxir administration had opposing effects on these 2 variables, resulting in no significant etomoxir-induced change in  $R_f^*$  in most tissues (Fig. 2). The exceptions were nonoxidative inguinal fat, where an increase in  $R_f^*$  reflected the plasma NEFA elevation, and highly oxidative heart, where the substantial decrease in clearance (6-fold in 18-h fasted rats) was translated into a decrease in absolute NEFA uptake.

**Insulin administration.** Results derived from 5-h fasted hyperinsulinemic rats are shown in all figures as a solid bar. The symbol § over this column indicates a significant difference between insulin-treated and untreated 5-h fasted rats.

Exogenous insulin administration elevated plasma insulin levels to the high physiological range (Table 1), and there was a marked fall in plasma NEFA concentration (Fig. 1). Elevation of plasma insulin levels also produced a significant decrease in whole-body NEFA turnover (Fig. 1) and total NEFA uptake in most of the tissues studied (Fig. 2). The mass-action effect of the large fall in plasma NEFA concentration (Fig. 1) would be expected to contribute significantly to this response. However, clearance of  $^3\text{H-R-BrP}$  was increased in white and brown adipose tissue and in white quadriceps and was decreased in heart (Fig. 3), suggesting that mechanisms other than mass action may be modulating NEFA uptake in a tissue-specific manner.

**Comparison of analog and authentic tracer.** Etomoxir administration allowed a valid comparison of  $^3\text{H-R-BrP}$  and  $^{14}\text{C-P}$  in the conscious state. Under conditions of oxidation blockade, similar behavior of the analog and authentic NEFA would be expected, since  $^3\text{H-R-BrP}$  is not a substrate for oxidation. Comparisons of the behavior of  $^{14}\text{C-P}$  and  $^3\text{H-R-BrP}$  tracers are shown in Fig. 4 and Table 2. In Fig. 4, clearance estimates for diaphragm are divided into 2 groups, with solid points derived from rats whose oxidation is impaired. In

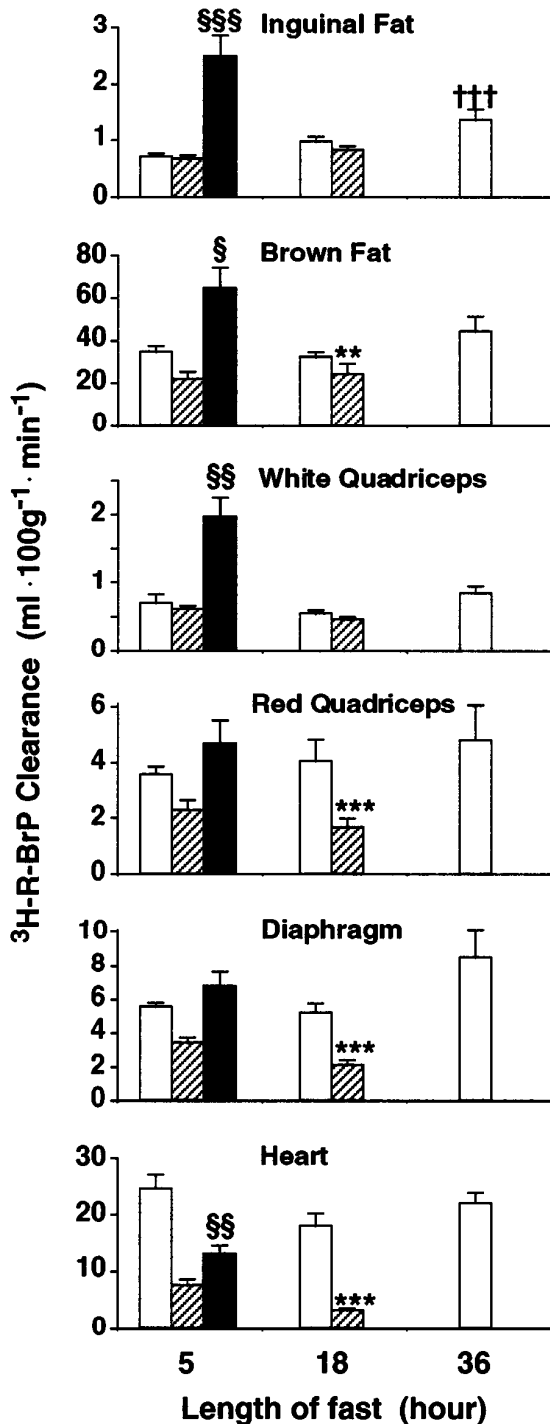


FIG. 3. Tissue clearance ( $K_f^*$ ) of  $^3\text{H-R-BrP}$  tracer in fasted but otherwise untreated rats (□), etomoxir-treated rats (▨) and hyperinsulinemic rats (■). \*, †, and § indicate a significant effect of etomoxir administration, fasting, and hyperinsulinemia, respectively. § $P < 0.05$ ; \*\*,\$§ $P < 0.01$ ; \*\*\*,†††,§§§  $P < 0.001$ .

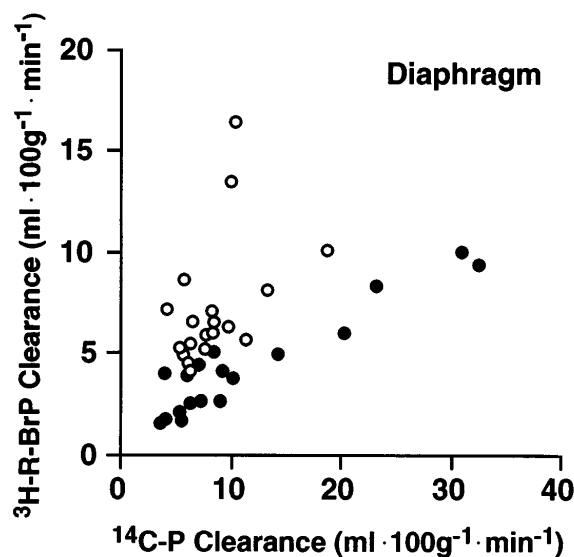


FIG. 4. Comparison of clearance estimates derived from  $^3\text{H-R-BrP}$  and  $^{14}\text{C-P}$  accumulation in diaphragm. ●, Situations where oxidation was substantially impeded [Fast (5 h) + Etx, Fast (18 h) + Etx, and Fast (5 h) + Ins]. For this restricted dataset,  $R^2 = 0.88$ . ○, All other cases where there was no obstruction to tissue loss of  $^{14}\text{C}$  via oxidation. Summary of similar data for other tissues is found in Table 2.

addition to etomoxir treatment, clamp data are also included in this group because acceleration of glucose uptake by hyperinsulinemia indirectly inhibits NEFA oxidation (14). All other data, from fasted but untreated rats, are shown as open points. These data generally lie above the oxidation-impaired points consistent with a greater loss of  $^{14}\text{C}$  label from the tissue through oxidation. An excellent correlation ( $R^2 = 0.88$ ) was evident between clearance estimates for  $^{14}\text{C-P}$  and  $^3\text{H-R-BrP}$  when oxidation was impeded (solid points). A significantly weaker relationship was observed ( $R^2 = 0.23$ ) when all data were included.

A summary of similar correlation analyses for all tissues is shown in Table 2. For the oxidative tissues (brown adipose tissue, red quadriceps, diaphragm, and heart), a stronger correlation between clearance estimates for the 2 tracers ( $K_f^*$  and  $K_{fs}'$ ) was evident when tissue oxidation was impeded. Highly significant relationships ( $R^2 = 0.62\text{--}0.97$ ,  $P < 0.0001$ ) were

obtained for all tissues. Overall, these results confirm that when conditions allow a comparison (i.e., when there is little loss of  $^{14}\text{C}$  from tissues through oxidation),  $^3\text{H-R-BrP}$  is a suitable substitute for  $^{14}\text{C-P}$  to monitor NEFA tissue utilization. Note that NEFA oxidation may not have been completely inhibited in the hyperinsulinemic group, but this would have diminished the power of the above analysis and would therefore not invalidate the above conclusions.

Also included in Table 2 are the tracer clearance ratios  $K_f^*/K_{fs}'$  for etomoxir-treated rats. Data obtained under clamp conditions were not included in these calculations, because there may have been residual oxidative capacity under these circumstances. The  $K_f^*/K_{fs}'$  ratios are estimates of the "lumped constant" used to scale  $^3\text{H-R-BrP}$  results to absolute indices of NEFA uptake or clearance if required. These are appropriate values to use in the conscious state.

## DISCUSSION

The experiments described here are the first application, in conscious animals, of a newly developed  $^3\text{H-R-BrP}$  technique (5) for the study of NEFA metabolism in laboratory animals. We report simultaneous measurements of NEFA uptake by a broad range of tissues studied in the postabsorptive or fasted states. Two interventions, etomoxir administration and insulin elevation, both known to modify lipid metabolism, were also studied here. Whole-body effects of fasting and treatments were as expected, but novel tissue-specific alterations in fatty acid metabolism were exposed.

In the postabsorptive state, the total rate of NEFA uptake into an individual tissue was generally matched by its oxidative capacity, as has been suggested by previous *ex vivo* work (15). In muscle, there were several orders of magnitude difference in NEFA uptake for nonoxidative white quadriceps muscle ( $0.28 \pm 0.06 \mu\text{mol} \cdot 100 \text{g}^{-1} \cdot \text{min}^{-1}$ ) and highly oxidative heart tissue ( $10.0 \pm 2.2 \mu\text{mol} \cdot 100 \text{g}^{-1} \cdot \text{min}^{-1}$ ) under basal conditions. Results for the oxidative red muscles studied (red quadriceps and diaphragm) fell between these 2 extreme values (Fig. 2). The same dependence of NEFA uptake on oxidative capacity was observed in different adipose tissues. Total uptake rates into oxidative brown adipose tissue ( $14.8 \pm 3.0 \mu\text{mol} \cdot 100 \text{g}^{-1} \cdot \text{min}^{-1}$ ) exceeded those in heart; values for nonoxidative inguinal fat ( $0.29 \pm 0.06 \mu\text{mol} \cdot 100 \text{g}^{-1} \cdot \text{min}^{-1}$ ) were comparable to rates in white muscle. After incorporating lumped-constant corrections (see below), these val-

TABLE 2  
Lumped constant estimates

Tissue	$R^2$ (inclusive)	$R^2$ (restricted)	Lumped constant ( $\text{LC}^* = K_f^*/K_{fs}'$ )
Inguinal fat	0.67	0.77	$0.37 \pm 0.02$
BAT	0.84	0.97*	$0.44 \pm 0.01$
White quadriceps	0.80	0.93	$0.45 \pm 0.03$
Red quadriceps	0.35	0.81*	$0.50 \pm 0.07$
Diaphragm	0.23	0.88†	$0.45 \pm 0.05$
Heart	0.05	0.62‡	$0.26 \pm 0.03$

$R^2$  (inclusive) is the coefficient of determination relating clearance estimates for  $^3\text{H-R-BrP}$  and  $^{14}\text{C-P}$  for all data. To calculate  $R^2$  (restricted), only cases where oxidation was substantially impeded [Fast (5 h) + Etx, Fast (18 h) + Etx, and Fast (5 h) + Ins] were included.  $\text{LC}^*$  is the clearance ratio for the 2 tracers ( $^3\text{H-R-BrP}/^{14}\text{C-P}$ ) using data from etomoxir-treated animals only. All  $R^2$  (restricted) are significantly different from zero ( $P < 0.0001$ ). Symbols indicate a significant difference between inclusive and restricted estimates of  $R^2$ . \* $P < 0.05$ , † $P < 0.001$ , ‡ $P < 0.01$ . Differences were assessed from *z*-transforms of  $R$  (28).

ues represent actual NEFA utilization rates of  $0.62 \pm 0.13$ ,  $38.5 \pm 8.5$ ,  $33.6 \pm 6.8$ , and  $0.78 \pm 0.16 \mu\text{mol} \cdot 100 \text{g}^{-1} \cdot \text{min}^{-1}$  for white quadriceps, heart, brown adipose tissue, and inguinal fat, respectively.

Fasting increased whole-body NEFA turnover, which was reflected by greater NEFA uptake by most tissues. Except for white adipose tissue, there was no change in NEFA tissue clearance, indicating that increased tissue and whole-body uptake was due mainly to elevated plasma NEFA concentrations resulting from increased lipolysis. The singular observation that  $^3\text{H-R-BrP}$  clearance by white fat increased with fasting (Fig. 3) may indicate augmentation of NEFA re-esterification (16) or could be due (in part) to countercurrent influx (17) coupled to accelerated NEFA outflow from adipocytes. Whatever the responsible mechanism, the observed uptake of NEFA by adipose tissue would have only a small effect on whole-body NEFA balance. If we assume that inguinal fat is typical of all white adipose tissue and use previously published body composition data (18), then the total NEFA influx into all fat beds represents only 3 and 5% of whole-body NEFA turnover after a 5- and 36-h fast, respectively.

The response to pharmacological blockade of  $\beta$ -oxidation (acute etomoxir administration) confirmed the close association between total NEFA uptake and its subsequent oxidation that was implied by the postabsorptive results. Etomoxir reduced NEFA clearance in oxidative tissues (brown fat, red quadriceps, diaphragm, and heart) but not in nonoxidative tissues (inguinal fat and white quadriceps). The rapid decrease in NEFA clearance with inhibition of  $\beta$ -oxidation indicates a close association between NEFA uptake and oxidation and suggests that the early steps of fatty acid uptake are closely coupled to the transfer of fatty acids to the mitochondrion. This contrasts with glucose metabolism, for which inhibition of glucose oxidation by infusion of fatty acids (19–21) does not immediately decrease glucose uptake, but diverts glucose metabolism to lactate or glycogen formation.

Comparison of the tissue accumulation of both  $^3\text{H-R-BrP}$  and  $^{14}\text{C-P}$  after etomoxir administration also verified that the uptake of bromopalmitate paralleled the uptake of authentic palmitate in conscious animals. The correlation between the clearance of bromopalmitate and authentic substrate under conditions of no fatty acid oxidation (Fig. 4) indicates that  $^3\text{H-R-BrP}$  accurately traces palmitate uptake. Pharmacological blockade of lipid oxidation also allowed the calculation of a set of lumped constants (Table 2) for adjusting NEFA uptake values (derived from  $^3\text{H-R-BrP}$  clearance) to actual fatty acid uptake in the conscious state. Values are typically 30% higher than those previously reported in barbiturate-anesthetized rats (5). The equivalent parameter, used to convert uptake results from deoxyglucose analogs to those for authentic glucose, is also known to vary slightly across different physiological conditions (22). Anesthesia has been shown to disturb specific aspects of lipid metabolism (23) and is also likely to have more general effects through modulation of catecholamine levels (24). It is therefore not surprising that a small difference between the lumped constant for  $^3\text{H-R-BrP}$  in conscious and anesthetized states was observed.

At the whole-body level, elevation of circulating insulin levels had the opposite effect of fasting. This state was associated with reduced plasma NEFA, reduced whole-body NEFA turnover, and a corresponding reduction in NEFA uptake into most tissues, implying that reduced NEFA supply

played a large part in alterations of tissue NEFA uptake in response to insulin. However, unlike the changes associated with fasting, NEFA clearance was altered in some lipid-utilizing tissues, indicating modification of the processes involved in the uptake and/or metabolic sequestration of NEFA. The direction of the response was not uniform across tissues. In nonoxidative tissues, such as white fat and white muscle, an increase in  $^3\text{H-R-BrP}$  clearance was observed; in highly oxidative heart tissue, NEFA clearance decreased with physiological hyperinsulinemia.

Reduced substrate competition alone would tend to increase clearance of NEFA, considering that hyperinsulinemia lowered plasma NEFA concentrations to below the apparent  $K_m$  for the NEFA oxidation and storage processes (25). Human studies suggest that the magnitude of such an effect could be large. The insulin-stimulated increase in whole-body clearance of NEFA observed when plasma NEFA levels were (as here) allowed to fall was absent when plasma NEFA concentrations were maintained at preclamp values (9). However, it is also likely that insulin directly promotes lipid storage (tending to increase  $^3\text{H-R-BrP}$  clearance) by stimulating acylglyceride formation (26). In contrast, increased glucose oxidation induced by hyperinsulinemia indirectly inhibits tissue lipid oxidation (presumably by elevation of cytosolic malonyl-CoA) (14). Estimates of  $^3\text{H-R-BrP}$  clearance shown in Fig. 3 reflect both oxidation and storage processes, which were subjected to competing influences. The balance achieved depended on the oxidative capacity of individual tissues. In adipose tissues and the nonoxidative white quadriceps, storage appears to be the dominant process, with total NEFA clearance increasing with physiological hyperinsulinemia. Highly oxidative heart muscle apparently responded predominantly to blockade of the oxidation pathway, resulting in a decrease in  $^3\text{H-R-BrP}$  clearance in this tissue. It is likely that the 2 opposing effects approximately balanced in red quadriceps and diaphragm.

The responses to hyperinsulinemia and etomoxir administration illustrate that the ability to simultaneously determine NEFA uptake in several tissues with a range of oxidative capacities provides additional insight into the mechanistic detail of these interventions. It is evident that most of the observed changes in NEFA uptake result from the net effect of 2 (or more) possibly opposing primary effects. For example, as discussed above, it is likely that insulin simultaneously acts to lower plasma NEFA by suppressing lipolysis, increasing intracellular lipid storage, and indirectly reducing NEFA oxidation. In the case of etomoxir, the balance was between direct and indirect effects in different tissues. Here an elevation of circulating NEFA levels (induced by reduced clearance in oxidative tissues) tended to increase absolute NEFA uptake into all (including nonoxidative) tissues. These separate actions become apparent only when multiple tissues with different metabolic properties are studied simultaneously. Moreover, although these basic effects can be studied in other systems (e.g., *in vitro* preparations), the exact balance between them, attained in a specific tissue under specific physiological conditions, can only be determined by direct measurement *in vivo*.

The initial validation studies of the newly developed  $^3\text{H-R-BrP}$  technique were conducted in anesthetized rats (5). The present results, obtained in conscious animals, credibly demonstrate that the methodology provides reliable information over a more extensive range of physiological and

pharmacological conditions. However, as with all new techniques, caution must be exercised, and ongoing evaluation of results is required to identify conditions under which the methodology may have limitations and/or require modification. Moreover, we do not necessarily regard the technique as static; better identification of the tissue metabolites of the authentic and analog NEFA tracers, which could lead to a refinement of the methodology, remains a high priority.

Until recently, it has been a generally held view that tissue NEFA utilization is driven predominantly by systemic supply (7). However, indirect evidence is now emerging (based on changes in expression of molecules involved in transport and early metabolic steps [27]) that local tissue control mechanisms may also regulate NEFA uptake and utilization. The absence of methodology to study NEFA metabolism in vivo at the individual tissue level has precluded a rigorous functional evaluation of such putative control mechanisms. The development of the  $^3\text{H}$ -R-BrP tracer methodology has enabled, for the first time, an exploration of NEFA metabolism in a broad range of tissues across metabolic states with diminished or enhanced lipid oxidation. We have shown here that the early steps of NEFA uptake can be rapidly regulated by its rate of oxidation.

We are cautiously confident that future studies using  $^3\text{H}$ -R-BrP will contribute to our understanding of fuel metabolism in health and disease. The technique has special relevance to the study of type 2 diabetes, given the well-established relationship between disturbed lipid and carbohydrate metabolism in insulin resistance. This could be of particular importance for the development and evaluation of therapies that are thought to act via redistribution of lipid stores or alteration of lipid metabolism.

#### ACKNOWLEDGMENTS

Work performed at the Garvan Institute was supported by the National Health and Medical Research Council of Australia and by AstraZeneca, Sweden.

From the Garvan Institute, we thank Donna Wilks for her expert surgery and all staff of the Biological Testing Facility for their care and preparation of animals. At AstraZeneca, we gratefully acknowledge the expert technical assistance of Pia Thalén and Ann Kjellstedt. We are also indebted to Maria Ölwegård-Halvarsson and Roger Simonsson for the synthesis and resolution of [9,10- $^3\text{H}$ ]- (R)-2-bromopalmitate tracer.

#### REFERENCES

1. Goodpaster BH, Kelley DE: Role of muscle in triglyceride metabolism. *Curr Opin Lipidol* 9:231–236, 1998
2. Kraegen EW, Cooney GJ: The role of free fatty acids in muscle insulin resistance. In *Diabetes Annual*. Marshall SM, Home PD, Rizza RA, Eds. Amsterdam, Elsevier Science, 1999, p. 141–159
3. Boden G: Role of fatty acids in the pathogenesis of insulin resistance and NIDDM. *Diabetes* 46:3–10, 1997
4. Declercq PE, Falck JR, Kuwajima M, Tyminski H, Foster DW, McGarry JD: Characterization of the mitochondrial carnitine palmitoyltransferase enzyme system. I. Use of inhibitors. *J Biol Chem* 262:9812–9821, 1987
5. Oakes ND, Kjellstedt A, Forsberg G-B, Clementz T, Camejo G, Furler SM, Kraegen EW, Ölwegård-Halvarsson M, Jenkins AB, Ljung B: Development and initial evaluation of a novel method for assessing tissue-specific plasma free fatty acid utilization in vivo using (R)-2-bromopalmitate tracer. *J Lipid Res* 40: 1155–1169, 1999
6. Maki MT, Haaparanta M, Nuutila P, Oikonen V, Luotolahti M, Eskola O, Knuuti JM: Free fatty acid uptake in the myocardium and skeletal muscle using fluorine-18-fluoro-6-thia-heptadecanoic acid. *J Nucl Med* 39:1320–1327, 1998
7. Coppack S, Jensen M, Miles J: In vivo regulation of lipolysis in humans. *J Lipid Res* 35:177–193, 1994
8. Cahill GF, Herrera MG, Morgan AP, Soeldner JS, Steinke J, Levy PL, Reichard GA, Kipnis DM: Hormone-fuel interrelationships during fasting. *J Clin Invest* 45:1751–1769, 1966
9. Groop LC, Bonadonna RC, Shank M, Petrides AS, DeFronzo RA: Role of free fatty acids and insulin in determining free fatty acid and lipid oxidation in man. *J Clin Invest* 87:83–89, 1991
10. Schulz H: Inhibitors of beta-oxidation. *Prog Clin Biol Res* 321:153–165, 1990
11. Clark PW, Jenkins AB, Kraegen EW: Pentobarbital reduces basal liver glucose output and its insulin suppression in rats. *Am J Physiol* 258:E701–E707, 1990
12. Kraegen EW, James DE, Bennett SP, Chisholm DJ: In vivo insulin sensitivity in the rat determined by euglycemic clamp. *Am J Physiol* 245:E1–E7, 1983
13. Hagenfeldt L: A gas chromatographic method for the determination of individual free fatty acids in plasma. *Clin Chim Acta* 13:266–268, 1966
14. Sidossis LS, Stuart CA, Shulman GI, Lopaschuk GD, Wolfe RR: Glucose plus insulin regulate fat oxidation by controlling the rate of fatty acid entry into the mitochondria. *J Clin Invest* 98:2244–2250, 1996
15. Dyck DJ, Peters SJ, Glatz J, Gorski J, Keizer H, Kiens B, Liu S, Richter EA, Spriet LL, van der Vusse GJ, Bonen A: Functional differences in lipid metabolism in resting skeletal muscle of various fiber types. *Am J Physiol* 272: E340–E351, 1997
16. Carlson MG, Snead WL, Campbell PJ: Fuel and energy metabolism in fasting humans. *Am J Clin Nutr* 60:29–36, 1994
17. Lieb WR, Stein WD: Testing and characterizing the simple carrier. *Biochim Biophys Acta* 373:178–196, 1974
18. Storlien LH, James DE, Burleigh KM, Chisholm DJ, Kraegen EW: Fat feeding causes widespread in vivo insulin resistance, decreased energy expenditure, and obesity in rats. *Am J Physiol* 251:E576–E583, 1986
19. Jenkins AB, Storlien LH, Chisholm DJ, Kraegen EW: Effects of nonesterified fatty acid availability on tissue-specific glucose utilization in rats in vivo. *J Clin Invest* 82:293–299, 1988
20. Kruszynska YT, McCormack JG, McIntyre N: Effects of glycogen stores and non-esterified fatty acid availability on insulin-stimulated glucose metabolism and tissue pyruvate dehydrogenase activity in the rat. *Diabetologia* 34:205–211, 1991
21. Park JY, Kim CH, Hong SK, Suh KI, Lee KU: Effects of FFA on insulin-stimulated glucose fluxes and muscle glycogen synthase activity in rats. *Am J Physiol* 275:E338–E344, 1998
22. Ng CK, Holden JE, DeGrado TR, Raffel DM, Kornguth ML, Gately SJ: Sensitivity of myocardial fluorodeoxyglucose lumped constant to glucose and insulin. *Am J Physiol* 260:H593–H603, 1991
23. Mortimer BC, Umeda Y, Elsegood CL, Redgrave TG: Effects of anaesthesia on the removal from plasma of intravenously injected chylomicron-like lipid emulsions in rats and mice. *Clin Exp Pharmacol Physiol* 20:51–58, 1993
24. Baum D, Halter JB, Taborsky GJ Jr, Porte D Jr: Pentobarbital effects on plasma catecholamines: temperature, heart rate, and blood pressure. *Am J Physiol* 248:E95–E100, 1985
25. Luiken JJ, van Nieuwenhoven FA, America G, van der Vusse GJ, Glatz JF: Uptake and metabolism of palmitate by isolated cardiac myocytes from adult rats: involvement of sarcolemmal proteins. *J Lipid Res* 38:745–758, 1997
26. Vila MC, Milligan G, Standaert ML, Farese RV: Insulin activates glycerol-3-phosphate acyltransferase (de novo phosphatidic acid synthesis) through a phospholipid-derived mediator: apparent involvement of G $\alpha$  and activation of a phospholipase C. *Biochemistry* 29:8735–8740, 1990
27. Bonen A, Dyck DJ, Luiken JJ: Skeletal muscle fatty acid transport and transporters. *Adv Exp Med Biol* 441:193–205, 1998
28. Sokal RR, Rohlf FJ: *Biometry: The Principles and Practice of Statistics in Biological Research*. San Francisco, Freeman, 1969, p. 515–523